

THEORETICAL AND OBSERVATIONAL CONSTRAINTS ON LUNAR MEGA-REGOLITH THICKNESS. Jonathan Besserer, Francis Nimmo, *Dept. Earth & Planetary Sciences, U.C. Santa Cruz, Santa Cruz CA 95064, USA (jbessere@ucsc.edu)*, Mark A. Wieczorek, *Institut de Physique du Globe de Paris, 94100 Saint-Maur-des-Fossés, France*, Walter S. Kiefer, *Lunar and Planetary Institute, 3600 Bay Area Blvd, Houston TX 77058, USA*, Jeff Andrews-Hanna, *Dept. Geophysics, Colorado School of Mines, Golden, CO 80401, USA*, Maria T. Zuber, *Department of Earth, Atmospheric and Planetary Sciences, Massachusetts Institute of Technology, Cambridge, MA 02129, USA*.

Introduction Recent GRAIL results suggest that at least the top few km of the lunar crust (the mega-regolith) have lower density than expected, indicating porosities of order 10 % [1]. Porosity at depth will close at a rate dependent on temperature and overburden pressure [2]. High-resolution GRAIL measurements [3] can potentially map the thickness of this layer, providing a constraint on the time-temperature history of the crust.

Pore closure

To model pore closure, we solve two coupled equations:

$$\frac{d\phi}{dt} = -\phi \frac{P}{\eta} \quad (1)$$

and

$$\rho C_p \frac{\partial T}{\partial t} = \frac{\partial}{\partial z} \left(k \frac{\partial T}{\partial z} \right) + H \quad (2)$$

where the first equation describes the evolution of porosity ϕ [2] and the second describes the evolution of temperature T . The two equations are coupled because the thermal conductivity k is a function of ϕ [4], while the viscosity η is a function of T . Here P is the overburden pressure, ρ is the density, C_p the specific heat capacity, and H the internal heat generation rate.

To frame the problem in a tractable manner, this approach assumes that there are no processes that regenerate porosity. At the crustal-scale depths that can be probed by GRAIL's high-resolution gravity [3], this assumption should be roughly correct for the Moon subsequent to late heavy bombardment. Our approach calculates the maximum porous layer thickness; the actual porous layer thickness may be smaller depending on the processes (e.g., ejecta blanket emplacement [5]) that initially generated porosity. Our approach also neglects other processes, such as volcanism, that might cause local annealing of pores [6].

We assume that crustal heat generation occurs at a rate $H = \sum_i H_{0,i} \exp(-\lambda_i t)$, where $H_{0,i}$ is a free parameter and λ_i is the decay constant of the i -th isotope, assuming a K:Th:U ratio of 2000:3.7:1 [7]. $H_{0,i}$ is assumed to vary vertically, with an exponential decay length of 20 km [7]. We fix the surface temperature at T_s and specify the heat flux into the base of the crust: $F_b = F_{now} \exp(\beta[t_{now} - t])$, where F_{now} is the present-day assumed mantle heat flux of $4.6 \text{ mW} \cdot \text{m}^{-2}$ [7], t_{now} is 4.5 Gyr, and β is a free parameter describing how the heat flux has evolved over time. The crust is assumed to be 45 km thick [1] and to have the rheology of dry anorthite [8].

Model results typically show porosity decaying to zero over a narrow depth range [1]. Figure 1 plots the maximum porous layer thickness for an initial porosity $\phi_0 = 10 \%$ after 3.9 Gyr evolution. Note that the major part of the evolution

occurs in the first tens of Myrs. The rate of internal heating $H_{0,i}$ is parameterized according to the implied surface Th concentrations, while the mantle decay constant β is plotted in terms of the initial heat flux implied. Higher mantle heat fluxes and higher Th concentrations result in a thinner porous layer. A smaller crustal decay length would permit a thicker porous layer. Porosity at depths of several tens of km can survive for 3.9 Gyr for most parameter combinations.

These plots provide three predictions for porous maximum layer thickness that can potentially be tested with GRAIL observations (see below). Other things being equal: 1) Near the poles, the porous layer will be thicker because of lower surface temperatures; 2) Higher surface Th concentrations imply thinner porous layers; 3) Higher initial porosities imply thinner porous layers (because of the reduced thermal conductivity). Thus, for instance, the margins of the Procellarum Creep Terrane (PKT) have high Th concentrations [9] and high surface porosity [1], implying that the porous layer there should be thin.

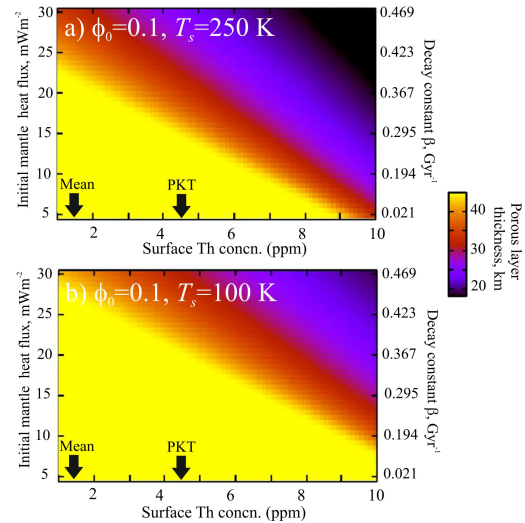


Figure 1: Maximum thickness of porous layer after 3.9 Gyr, calculated using the method described in the text and assuming an initial porosity $\phi_0 = 10 \%$. Initial mantle heat flux refers to the value at 3.9 Gyr B.P. The present day value is taken to be $4.6 \text{ mW} \cdot \text{m}^{-2}$ and exponential decay with a decay constant β is assumed. Crustal heat production is calculated based on surface Th concentration (see text). Arrows mark mean observed surface Th concentration and that typical of the PKT [9]. a) Surface temperature 250 K (i.e. equator). b) Surface temperature 100 K (i.e. poles).

Admittance

To determine the actual thickness of the porous layer, we use an admittance approach. Consider two sinusoidal interfaces, separated by a mean distance t_u and with a phase offset Φ (see Figure 2). The density contrasts at the upper and lower interfaces are ρ_u and $\Delta\rho = \rho_l - \rho_u$, respectively, the topographic amplitudes are h_0 and h_1 , and the interfaces are presumed to be rigidly supported.

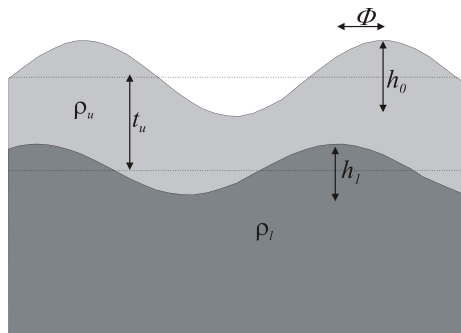


Figure 2: Definition sketch.

Neglecting sphericity and finite-amplitude corrections, at short wavelengths the surface gravity anomalies due to the upper and lower interfaces are respectively

$$\Delta g_u = 2\pi G \rho_u h_0 \cos(kx) \quad (3)$$

and

$$\Delta g_l = 2\pi G \Delta\rho h_1 e^{-kt_u} \cos(kx + \Phi). \quad (4)$$

Here G is the gravitational constant, x is the horizontal coordinate, and k is the wavenumber.

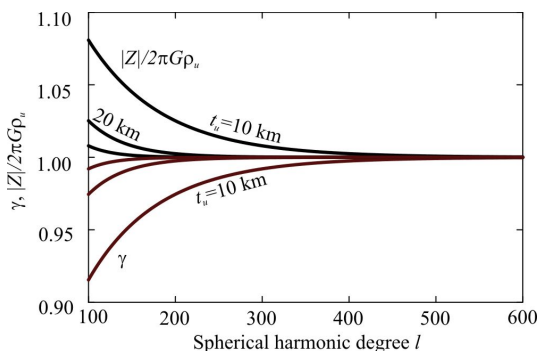


Figure 3: Variation of admittance $|Z|$ and correlation γ as a function of spherical harmonic degree l and porous layer thickness t_u , calculated assuming the phase offset Φ is randomly distributed. Here the quantity $\frac{h_1}{h_0} \frac{\Delta\rho}{\rho_u} = 1$ and $t_u = 10, 20, 30$ km.

The magnitude of the ratio of the net surface gravity anomaly to the surface topography, referred to as the admittance $|Z|$, is given by

$$|Z| = 2\pi G \rho_u [1 + f_u^2 + 2f_u \cos \Phi]^{1/2} \quad (5)$$

where $f_u = \frac{h_1}{h_0} \frac{\Delta\rho}{\rho_u} e^{-kt_u}$. If the two interfaces are in-phase ($\cos \Phi = 1$) then the gravity contributions add, while if they are in anti-phase, they subtract. The quantity f_u compares the contribution of the lower interface with the upper interface; upwards attenuation reduces the contribution of the lower interface.

We define the correlation between gravity and surface topography as

$$\gamma = \frac{\overline{h\Delta g}}{\sqrt{\overline{h^2}} \sqrt{\overline{\Delta g^2}}} \quad (6)$$

where overlines represent the expected value; this definition allows for positive and negative values of γ . It can then be shown that

$$\gamma = \frac{(1 + f_u \cos \Phi)}{(1 + f_u^2 + 2f_u \cos \Phi)^{1/2}}. \quad (7)$$

In the limit of no signal from the interface ($f_u = 0$) then the correlation is 1, as required. If the two interfaces are in phase ($\Phi = 0$) then $\gamma = 1$, as required, while if the interfaces are in anti-phase the correlation is reduced and equals zero if $f_u = 1$ (because the two gravity signals exactly cancel each other out).

Assuming that the phase angle Φ is random and independent of wavenumber, then the ensemble average admittance and correlation can be calculated by integrating equations (5) and (7) over Φ . Figure 3 plots the results for $|Z|$ and γ as a function of spherical harmonic degree for three different values of porous layer thickness t_u . At very short wavelengths the results are sensitive only to the properties of the porous layer. At longer wavelengths, depending on t_u , the properties of the lower layer become important; for instance, the admittance (or, equivalently, the effective density) increases because density of the lower layer is higher. GRAIL measurements should be able to resolve these kind of features of the gravity field.

References

- [1] Wieczorek M.A. et al., *Science Express*, 2012.
- [2] Nimmo, F. et al., *Icarus* 166, 21-32, 2003.
- [3] Zuber M. et al. (2013) LPSC, (this mtg).
- [4] Smoluchowski R. (1981) *Astrophys. J.* 244, L31.
- [5] Fassett C.I. et al., (2011) *GRL* 38, L17201.
- [6] Kiefer W.S. (in press), *J. Geophys. Res.*
- [7] Garrick-Bethell I. et al. (2010) *Science* 330, 949-951.
- [8] Rybacki E. and Dresen G. (2000) *JGR* 105, 26017-26036.
- [9] Jolliff B.L. et al. (2000) *JGR* 105, 4197-4216.